Vol. 33 (2002) ACTA PHYSICA POLONICA B No 10

PHOTON STRUCTURE FROM HERA*

Stephen Maxfield

On behalf of the H1 and ZEUS Collaborations

Dept. of Physics, University of Liverpool
Oxford Street, Liverpool L69 7ZE, UK

(Received July 18, 2002)

Some recent measurements of real and virtual photon structure at HERA are reviewed. The cross section for dijet events in photoproduction is compared to NLO QCD calculations. In low Q^2 DIS, the production of dijets is shown to be sensitive to the structure of longitudinally polarised photons and the Q^2 evolution modified in charm-enriched events.

PACS numbers: 13.60.Fz, 14.70.Bh

1. Introduction

Measurements of dijet production in photoproduction and low Q^2 Deep Inelastic Scattering (DIS) supply constraints on the parton density functions (pdf's) of real and virtual photons respectively as well as tests of perturbative QCD. This is because the jets can be produced in resolved photon interactions where the photon has fluctuated into a system of partons one of which undergoes a hard scattering with a parton from the proton. In effect the proton beam acts as a source of coloured partons which probe of the structure of the target photon. They do this at a scale determined by the transverse energy, E_{T} of the jets. The cross section for the process can be written as a convolution of photon fluxes, parton densities for the photon and proton and matrix elements for the parton–parton scattering:

$$\sigma \sim f_{\gamma^{*k}|e} \otimes \mathrm{pdf}^{\gamma,k} \otimes \mathrm{pdf}^{\mathrm{proton}} \otimes M_{ij}\,.$$

Of the various components, the photon fluxes, $f_{\gamma^{*k}|e}$, $k = \mathrm{T,L}$, are determined from QED, the matrix elements have been calculated up to NLO in perturbative QCD and parton densities in the proton have been measured

* Presented at the X International Workshop on Deep Inelastic Scattering (DIS2002) Cracow, Poland, 30 April–4 May, 2002.

to high precision from deep inelastic scattering data. Parton densities for quasi-real photons have been obtained from global fits to measurements of the photon structure function F_2^{γ} taken at several different scales in $e\gamma$ DIS (two photon) processes at e^+e^- colliders.

I will try to summarise the current status of photon structure measurements made at HERA concentrating on the more recent dijet cross section measurements made by ZEUS and H1. The analyses are presented individually and in more detail elsewhere in these proceedings [1]. Single-inclusive jet cross sections are also useful in this context but I will not discuss them here.

2. Real photon structure

H1 and Zeus have completed similar measurements of the high E_{T} dijet cross section in photoproduction [2]. The H1 measurement is based on an integrated luminosity of 34.9 pb^{-1} with inelasticity in the range $0.1 < y < 0.9$. A $\mathrm{k_t}$ algorithm [3] was used to find jets. Selected events contain at least two jets in the range $-0.5 < \eta < 2.5$ with asymmetric cuts on their transverse energy, $E_{\mathrm{T}}^{\mathrm{jet1}} > 25\,\mathrm{GeV}$ and $E_{\mathrm{T}}^{\mathrm{jet2}} > 15\,\mathrm{GeV}$. The measured cross sections are compared with next-to-leading order QCD calculations [4]. Effects of hadronisation are estimated with leading order simulations (HERWIG 5.9 [5] and PYTHIA 5.7 [6]). The calculations use GRV-HO and AFG-HO densities for the photon and CTEQ5M densities for the proton.

The ZEUS measurement was made using slightly different inelasticity ranges (134 GeV $< W_{\gamma p} <$ 277 GeV) and the jets were limited to $-1.0 < \eta < 2.4$ with $E_{\mathrm{T}}^{\mathrm{jet1}} > 14\,\mathrm{GeV}$ and $E_{\mathrm{T}}^{\mathrm{jet2}} > 11\,\mathrm{GeV}$. Comparisons are again made to the NLO calculations of Frixione *et al.*, corrected for hadronisation effects using HERWIG 6.1 (and PYTHIA 6.1).

The NLO matrix elements can be tested by looking at the distribution of the cosine of the centre of mass scattering angle, $\cos\theta^* = \tanh(\Delta\eta/2)$. This is controlled by the propagator: necessarily a quark in direct photon interactions and dominantly a gluon in resolved processes. Enriched samples of the two types of process can be obtained by selecting events according to the value of:

$$x_{\gamma,\mathrm{jets}} \equiv \frac{E_{\mathrm{T,jet1}}\mathrm{e}^{-\eta_{\mathrm{jet1}}} + E_{\mathrm{T,jet2}}\mathrm{e}^{-\eta_{\mathrm{jet2}}}}{2yE_{\mathrm{ebeam}}} \tag{1}$$

which $\rightarrow 1$ in direct events. A cut on the dijet mass is needed to avoid distortion of the distributions by phase space effects. Within the experimental and theoretical uncertainties, the NLO calculations give a good description of the distributions indicating that the dynamics of the dijet production mechanism are understood.

The NLO calculations use pdf's for real photons obtained from fits to $e\gamma$ scattering data. If these can also describe the *ep* data then this is an indication that universality holds. Conversely, the *ep* data can provide useful constraints on the pdf's in future fits. Figure 1 shows distributions of $x_{\gamma,\mathrm{jets}}$ from the two experiments. The NLO predictions agree well with the H1 data and give a marginal but still compatible description of the ZEUS data. At lower values of jet E_{T}, the NLO calculations tend to overestimate the ZEUS data. This may indicate a need for revision of the photon pdf's, however there are other factors contributing to the mismatch. Cuts on the E_{T} of the two jets are made asymmetrically because the NLO calculations need phase space for soft gluon radiation to cancel singularities and produce reliable predictions [7]. Figure 2(left) shows how the data and NLO calculations depend on $E_{\mathrm{T}}^{\mathrm{jet2}}$. The experiments choose different cuts on $E_{\mathrm{T}}^{\mathrm{jet2}}$. Although compatible within the large theoretical errors (dominated by the scale uncertainty) the shape seen in the data is not well described by the calculations (which are in any case expected to fail as the E_{T} approaches that of $E_{\mathrm{T}}^{\mathrm{jet1}}$) and explains why the H1 and ZEUS comparisons differ. The figure also shows the prediction from a leading order Monte Carlo (HERWIG) which includes parton showers. This agrees well with the data even where the jet E_{T}s become similar and is an indication that resummed NLO or NNLO calculations may be needed to fully describe this corner of phase space.

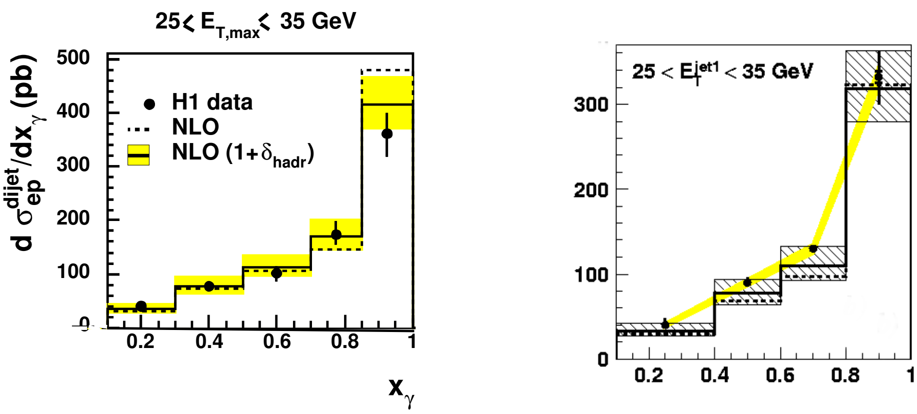

Fig. 1. Left: Distribution of x^{γ} in photoproduction as measured by H1. The data are compared with NLO predictions. Right: A similar measurement from ZEUS.

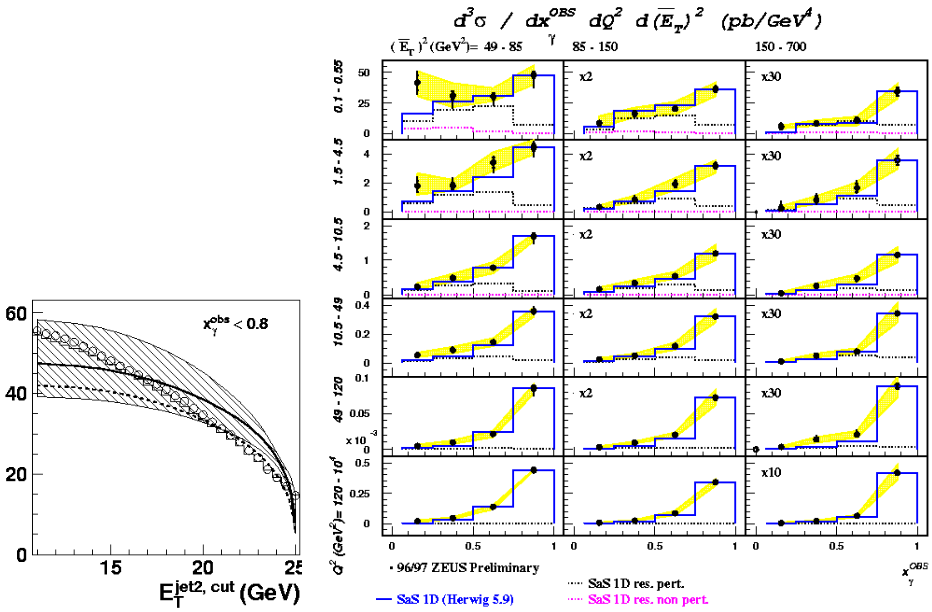

Fig. 2. Left: Dependence of the dijet cross section (points with error bars) on the transverse energy of the second jet and the behaviour of NLO prediction (solid line). The shaded band shows the scale uncertainty and the solid histogram is the (normalised) LO prediction from HERWIG. Right: The triple differential cross-section $d^3\sigma/dx_\gamma^{\rm OBS}dQ^2d(\overline{E}_{\rm T})^2$. The LO prediction from HERWIG5.9 with SaS 1D pdfs for the photon are also shown.

3. Virtual photon structure

If the 'target' photon is off-shell , *i.e.* in low DIS, the finite Q^2 provides a second hard scale. The leading log contributions to the cross section are now $\sim \ln\frac{E_{\rm T}^2}{Q^2}$ (rather than $\sim \ln\frac{E_{\rm T}^2}{\Lambda^2}$). Furthermore, for Q^2 large enough, the non-perturbative contributions to the γ^* structure (VDM) are strongly suppressed ($\sim \frac{1}{Q^4}$) relative to the calculable perturbative terms. This means that γ^* pdf's are not strictly required. The inclusion of virtual photon structure remains useful however as it extends fixed order calculations by resummation of near collinear terms and provides framework for a smooth transition from photoproduction to DIS.

H1 and ZEUS are extending previous studies of virtual photon structure. Figure 2(right) shows the distribution of $x_\gamma^{\rm OBS}$ measured by ZEUS for various ranges of Q^2 and the mean jet $\bar{E}_{\rm T}$. The data are compared with LO models using SaS1D [8] pdf's of the photon which take into account the expected evolution with photon virtuality. The normalisation of these models is uncertain and they have been scaled to the highest x_γ bin in each of the plots. The perturbatively calculable component dominates in all Q^2 and$\bar{E}_{\mathrm{T}}$ ranges and the resolved component is needed wherever $E_{\mathrm{T}}^2 > Q^2$. ZEUS observe a modification of the Q^2 evolution for charm enriched events in which the heavy quark mass provides a third hard scale. The Q^2 evolution, see figure 3(left), ceases when Q^2 drops below the charm threshold.

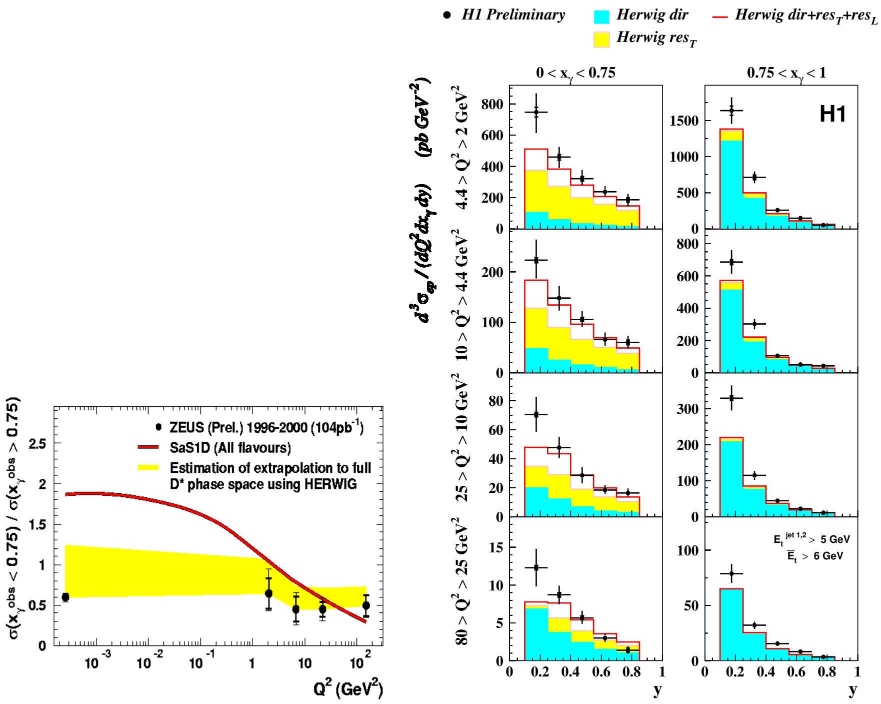

Fig. 3. Left: The ratio of resolved-like to direct-like events as a function of Q^2 for charm enriched events. Right: Dependence of the dijet cross section (points with error bars) on y for various x_γ and Q^2 ranges. The data are compared to LO Monte Carlo predictions with and without a $\gamma^{*\mathrm{L}}$ pdf.

Most models for virtual photon structure include only the transverse modes. Gauge invariance ensures that the $\gamma^{*\mathrm{L}}$ contributions must vanish as $Q^2 \to 0$. For off-shell photons, QCD improved calculations [9] for γ^*L predict hadron-like scaling behaviour in contrast to the $\ln E_{\mathrm{T}}^2/Q^2$ suppression of the transverse pdfs. Little is known experimentally about the structure of longitudinal photons. Because the photon fluxes, $f_{\gamma^{*\mathrm{L}}|e} \xrightarrow[y\to 1]{} 0$ and $f_{\gamma^{*\mathrm{L}}|e} \xrightarrow[y\to 0]{} f_{\gamma^{\mathrm{T}}|e}$, the y-dependence of the cross-sections can be used to investigate the importance of longitudinal terms. H1 have compared distributions of y with a version of HERWIG5.9, modified to include $\gamma^{*\mathrm{L}}$ pdfs (see figure 3(right)). The result is an improved description of the y dependence and an indication that it may in future be possible to extract longitudinal pdf's from the data.

Both experiments are attempting to compare data with NLO calculations of the jet cross-sections. It can be anticipated that the role of virtual photon pdf's will be partially supplanted by the higher order terms.

In conclusion, dijet cross-section measurements in photoproduction are of sufficient precision to constrain pdf's of real photons. These constraints would be tighter if NNLO/resummed calculations were available. Virtual photon structure shows sensitivity to longitudinal polarisation of photon. Comparison of data with NLO predictions including virtual photon structure is underway.

REFERENCES

[1] See talks by: A. Lupi, *Acta Phys. Pol.*, **B33**, 3105 (2002); G. Frising, *Acta Phys. Pol.*, **B33**, 3117 (2002); K. Sedlak, *Acta Phys. Pol.*, **B33**, 3129 (2002); M. Lightwood, *Acta Phys. Pol.*, **B33**, 3111 (2002).

[2] C. Adloff *et al.* [H1 Collaboration], accepted by *Eur. Phys. J.* **C** , (2001/2); S. Chekanov *et al.* [ZEUS Collaboration], *Eur. Phys. J.* **C23**, 615 (2002).

[3] S. Catani, Yu.L. Dokshitzer, B. Webber, *Nucl. Phys.* **B406**,187(1993); S.D. Ellis, D.E. Soper, *Phys. Rev.* **D48**, 3160 (1993).

[4] S. Frixione, Z. Kunszt, A. Signer, *Nucl. Phys.* **B467**, 399 (1096); S. Frixione, *Nucl. Phys.* **B507**, 295 (1997); S. Frixione, G. Ridolfi, *Nucl. Phys.* **B507**, 315 (1997).

[5] G. Marcesini *et al.*, *Comput. Phys. Commun.* **67**, 465 (1992).

[6] T.J. Sjöstrand, *Comput. Phys. Commun.* **82**, 74 (1994).

[7] S. Frixione, G. Ridolfi, *Nucl. Phys.* **B507**, 315 (1997).

[8] G.A. Schüler, T.J. Sjöstrand, *Phys. Lett.* **B376**, 193 (1996).

[9] J. Chýla, *Phys. Lett.* **B488**, 289 (2000).